Journal of Applied Polymer Science

Relevance of the acid–base approach in prediction of adhesion properties in two-component injection moulding

Eduard Kraus,[1] Sonja Horvat,[1] Christian Deubel,[1] Christian Staudigel,[1] Benjamin Baudrit,[1] Peter Heidemeyer,[1] Martin Bastian,[1] Irina Starostina,[2] Oleg Stoyanov[2]

[1]SKZ, German Plastics Center, Research and Development, Friedrich-Bergius-Ring 22, Wuerzburg 97076, Germany

[2]Kazan National Research Technological University, Karl Marx Street 68, Kazan, Republic of Tatarstan 420015, RussianFederation

Correspondence to: E. Kraus (E-mail: e.kraus@skz.de)

ABSTRACT: We demonstrate the use of innovative wetting method in prediction of the adhesion properties of biobased polymers for two-component injection moulding, taking into account the acid–base surface properties of joined materials. The measurements were carried out in accordance with modified Berger method by calculation of the difference in shortened acidity parameter ΔD_{short} between hard and soft component. Correlation factors up to 0.99 were observed between ΔD_{short} and peel force. In comparison to results obtained by conventional wetting methods, high potential for the selection of components with high interface adhesion and for prediction of the functionality by the acid–base approach was demonstrated. © 2015 Wiley Periodicals, Inc. J. Appl. Polym. Sci. **2016**, *133*, 43048.

KEYWORDS: biopolymers & renewable polymers; biomaterials; elastomers; molding; properties and characterization

Received 9 August 2015; accepted 13 October 2015

DOI: 10.1002/app.43048

INTRODUCTION

Multicomponent injection moulding is widely used as manufacturing process in plastics technology for the production of rigid-flexible composites. It involves moulding of engineering thermoplastics as hard component and thermoplastic elastomer as soft component. The hard–soft combinations of different polymeric materials enable the production of high quality plastic structures with unique characteristics that come from the properties of both polymers, e.g., high strength and modulus from the hard component and flexibility and vibrational adsorbing properties from the soft component.[1–4]

In recent years, particular attention has been devoted to application of biobased and biodegradable plastics in multicomponent injection moulding, which enabled the production of environmentally friendly composites.[5,6] However, rapid development of these materials resulted in difficulties in interaction examination of used components. It is widely accepted that performance in multicomponent injection moulding is ascribed to a strong interfacial adhesion generated through interactions between polymers. The unknown adhesion properties of developed materials limit their application because of the increased costs in examination of polymer interactions.[7]

The main problem in production of composites by multicomponent injection moulding is to enhance the adhesion between the polymers at their interface. Weak interactions on the interfaces between the polymeric components can lead to low mechanical properties or cracks of the final material by loading.[8] Therefore, an important issue in multicomponent processing is choosing of the hard–soft polymer pairs with desired strong interfacial adhesion.[5]

Commonly, different methods are used for explanation and prediction of the polymer interaction in multicomponent injection moulding. Surface energies of polymeric parts are considered as significant factor for interaction efficiency. Higher surface energy enables spreading one component on another during processing followed with the maximized interfacial interaction.[9,10]

It is well known that the wetting and the resulting adhesion represent very complex phenomena. The resulting adhesion between the polymeric pairs is controlled and optimized by varying the formulation, various technological factors as well as by surface treatment. However, it is also proved that the acid–base interactions play the significant role in the formation of interfacial forces between joining materials. The best interfacial

interactions can thereby be obtained if one of the materials has primarily acidic and the other basic properties.[11–14] Since the polymeric modification for the formation of the boundary surfaces in the polymeric compounds is an important process having specific properties, the proper selection of the necessary modifications can also be performed from the viewpoint of acid–base approach.

In this work, the use of wetting method in prediction of the adhesion properties of biobased polymers for two-component injection moulding is demonstrated, taking into account the acid–base properties of joined polymers. The results show also a possibility for selecting the right polymers for high adhesion properties.

THEORY

Wettability of the surface is of crucial importance for creating adhesive joints between polymers. The surface free energy (SFE) is physicochemical property of a surface and can be determined indirectly by wettability measurements. High value of the SFE and its polar part leads to the pronounced interactions between polymers, and the resulting adhesion between the joining partners is stronger. On the other hand, the poor wetting indicates a low interactions potential.[15]

Many theories describe relationships between the surface energetics and the strength of the polymer joints from interactive forces existing on the interfaces.[16–19] The major disadvantage of these and many other modern studies is that they only use acid or base models and ignore the fact that almost every substance may have certain bipolarity. All plastics up to polymers with macromolecular chains of saturated hydrocarbons possess both acidic and basic properties. However, according to indepth analysis and calculations of the acidic and basic parameters, the assumption that the polymer surfaces are monopolar is incomplete or incorrect.[20]

Traditional and common methods for determination of disperse and polar components of the SFE is the graphical method based on eq. (1) of Owens–Wendt:

$$W_a=\gamma_L(1+\cos\theta)=W^D+W^P=2\left(\sqrt{\gamma_S^D\gamma_L^P}+\sqrt{\gamma_L^D\gamma_S^P}\right) \quad (1)$$

where W_a, W^D, and W^P represent the thermodynamic work of adhesion and its dispersive and polar part, respectively, and γ_S correspond to the SFE of the measurement liquid and the solid, respectively, with superscripts D and P indicating dispersive and polar part of the SFE.[21]

Based on this equation, known values γ_L of test liquids and contact angle measurements are examined on the surface with linear approximation in coordinates $\sqrt{\gamma_L^P/\gamma_L^D}$ vs. $W_a/2\sqrt{\gamma_L^D}$ applied. The intersection of the curve with the ordinate describes the disperse component $\sqrt{\gamma_S^D}$, and the slope of the straight line as the polar component equal to $\sqrt{\gamma_S^P}$. The resulting sum of the amounts found from the graphs represents the geometric mean of an approximation of the total SFE of a material. Application of this graphical method for determination of components of the SFE provides reliable and reproducible results.

Another value used in characterization of adhesive performance of two polymers is the polar ratio calculated as ratio of the polar components of two solids. According to some authors, when polar parts of the SFE of two polymers have similar value, then the strongest joints are formed.[22,23] However, in many empirical studies, it was ascertained, that only the knowledge of the SFE, disperse or polar component is not entirely sufficient to predict the functionality of a polymer. The common methods for determination of the wetting properties of various materials as well as for further analysis show different quantitative characteristics.[22,24]

In the last two decades, significant advances have been made in the interpretation of interfacial adhesion between polymers by acid–base theory. According to this theory, not only hydrogen bonds are formed between substrates, but also bonds based on electron donor and electron accepting phenomena.[14,20]

In 1991, E. J. Berger suggested an amendment or extension of introduced graphical Owens–Wendt method.[25] In the Bergeŕs method, the surface acidity of polymeric and metallic materials is determined by seven different test liquids, two of which bear an acidic (aniline, formamide), two a basic character (phenol, glycerol), and rest are chosen randomly. First, the values of acid–base or polar component γ_S^{AB} from the individual interactions with two acids and two bases are determined the exact description for the six step calculation of the γ_S^{AB} values for chosen liquids is described in Ref. 25. The acids and bases used here have very similar values of γ_L^{AB} and Lifshitz–van der Waal or disperse component γ_L^{LW}. The difference in the values γ_S^{AB} of acids and bases, which can be calculated by the formula (2) represents the measure of the acidity or basicity of the surface and is referred to D, also known as acidity parameter:

$$D=2\left|\left(\sqrt{\gamma_S^{AB}(\text{Aniline})}+\sqrt{\gamma_S^{AB}(\text{Formamide})}\right)-\left(\sqrt{\gamma_S^{AB}(\text{Phenol})}+\sqrt{\gamma_S^{AB}(\text{Glycerol})}\right)\right| \quad (2)$$

The value $D>0$ corresponds to the acid and $D<0$ to the basic character of the surface.[25]

The parameter D enables reliable determination of the surface acidity, but there is a problem related to the spreading of the aniline and phenol on the substrate surface. Aniline and phenol have ow values of the SFE (43.2 mN/m and 40.4 mN/m, respectively) and the polar component (2.0 and 2.6 mN/m, respectively), resulting in difficulties in precise measurement of their contact angles. Because of this limit, a shortened version of the eq. (1) to a quantity D_{short} was introduced:

$$D_{short}=\sqrt{\gamma_S^{AB}(\text{Formamide})}-\sqrt{\gamma_S^{AB}(\text{Glycerol})} \quad (3)$$

The ability of materials to form adhesive joints is calculated by the reduced parameter ΔD_{short} calculated as the absolute difference in the acidity parameters of the adhesive and the substrate:

$$\Delta D_{short}=\left|D_{short}^{\text{soft comp.}}-D_{short}^{\text{hard comp.}}\right| \quad (4)$$

High values of ΔD_{short} relate to strong interactions of the components as well as to more durable joins. The parameter ΔD_{short} was proved and established in recent years for modified and

Table I. Characteristics of Materials

Sample	PLA	PLA/PBS	PLA Basis	TPE-E	TPE-S01	TPE-S02	TPE-U
Density (kg/m^3)	1240	1470	1300	1060	1100	1180	1140
Tensile yield strength (MPa)	62	50	40	10	7.2	5	n.a.
Melt flow rate (190°C, g/10 min)	35	24–28	7.5	9	n.a.	n.a.	n.a.
Heat distortion temperature (°C)	55	n.a.	51	n.a.	n.a.	n.a.	n.a.
Crystalline melt temperature (°C)	155–170	150–170	n.a.	160–190	n.a.	n.a.	n.a.
Glass transition temperature (°C)	55–60	55–60	n.a.	42	n.a.	n.a.	n.a.

unmodified polyethylene, rubber, and epoxy coatings of various metal substrates.[26–29] In this paper the shortened Berger method was used for all measurements in order to select the right combination with good adhesion and high resulting mechanical properties of hard–soft pairs.

EXPERIMENTAL

Materials

Combinations of polylactidic acid (PLA), polylactide based polymer (PLA Basis), polylactide modified with 20% talc, and polybutylene succinate (PLA/PBS) as hard components and thermoplastic copolyester (TPE-E), two styrene block copolymers modified for adhesion with polycarbonate (TPE-S01) and acrylonitrile butadiene styrene (TPE-S02), and biobased thermoplastic polyurethane (TPE-U) as soft components were were investigated (material characteristics are summarized in Table I). All materials were delivered in the form of granulates.

Moulding

Hard–soft combinations were produced using the injection moulding machine TM 1300/525 + 130L UNILOG B4 (Wittman Battenfeld GmbH & Co. KG). Proccesing parameters such as cycle and drying time, injection pressure, nozzle temperature and temperature of drying were chosen according to the protocol of materials and were in range of 48–102°C, 4–8 h, 612–1487 bar, 200–250°C, 60–80°C, respectively.

Topography Tests

Surface topography was analyzed by stylus profilometer MarSurf M 400 and SD 26 (Mahr GmbH) according to DIN EN ISO 3274:1998-04. Measurements were taken in two direction, one in the direction of mould filling (0°) and another one transversely (90°). Cutoff length (L_c) of 0.8 mm was selected in accordance to DIN EN ISO 4288:1998-04. Evaluation length (L_m) was set to five sampling lengths (0.8 × 5.0 mm) with the total length (L_t) of 5.6 mm. Information about the roughness of the material was given from calculation of arithmetic mean roughness (R_a), root mean square roughness (R_q), and mean peak-to-valley height (R_z). Roughness values were measured with a sensitivity of 0.2 μm. Topography was also analyzed by white light interferometer (WLI) WLI-MoB-100 26 at magnification objective 20× (numerical aperture 0.4) (OPM Messtechnik GmbH) in accordance to DIN EN ISO 4768:1998-05. For evaluation of R_a, R_q, and R_z, values of L_c, L_m, and L_t were the same as for the profilometer (0.8, 4.0, and 5.6 mm, respectively). Cut-off surface for measuring square roughness parameters sR_a, sR_q, and sR_z had dimensions of 0.8 × 0.8 mm, with the sampling surface of 4.0 × 0.8 mm (total 5.6 × 0.8 mm). Samples were also analyzed in two directions, as in the profilometry measurements.

Measurement of the Surface Free Energy

Drop shape analysis instrument DSA 30 (Kruess Optronic GmbH) was used for measuring the contact angle of test liquids diiodomethane, ethylene glycol, formamide, glycerol, and deionized water (all of p.a. purity) on the surface. The slope of the CMOS-camera was adjusted to the recommended angle of 2°, and the magnification factor was set at 200 pixels/mm. Contact angle was measured immediately after dosing the drop on the solid surface in the case of diiodmethane, ethylene glycol and water (DIN 55660-2: 2011-12) and after 2 min for the formamide and glycerine as suggested in Ref. 26. Drop basis was approximately 0.5 mm. Measurements were carried out at 23°C and relative humidity of 50% using shortened version of the Berger method described above.

Test Specimen

The 2C peel-test specimen was manufactured by 2-component injection moulding. Firstly the hard-component specimen with dimensions of 150.0 × 50.0 × 3.0 mm was injected and after cooling down the soft-component was overmoulded in the same cycle. For testing the adhesion in dependence of the flow path, the overmoulded length was 150 mm. The thickness of the hard- and soft-component can be changed due to different mould configurations. All trials were performed with a thickness of 3.0 mm for the hard and 2.0 mm for the soft-component, as shown in Figure 1.

Peel Force Test

Determination of peel force of hard–soft combinations was conducted in accordance to VDI-Guideline 2019 by device Z010 (Zwick Roell AG). The trolley peel testing was carried out with the roller angle of 90°. All measurements were performed in standard atmosphere according to ISO 291:2008 with an air temperature 23°C and relative humidity of 50%. In addition to the measuring of the traverse position of the tensile-test machine, the position of the test trolley running on a guide rail was measured. The peel force was determined as the average or maximum force [N] in the range from 20.0 to 120.0 mm of the peel-path in dependence to the fracture resp. force–curve shape, as shown in Figure 2.

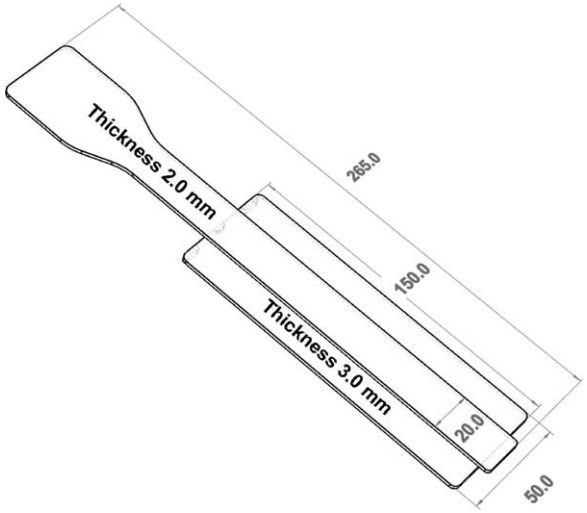

Figure 1. SKZ 2C peel-test specimen.

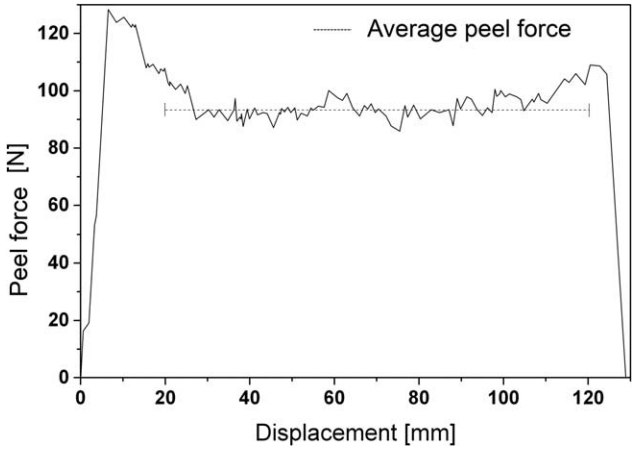

Figure 2. Determination of the peel force.

We studied only the samples that have shown on the entire test length a completely adhesive failure (AF) according to DIN EN ISO 10365.

RESULTS AND DISCUSSION

Topography Analysis

Results shown in Tables II and III show the linear roughness parameters for hard and soft components obtained by stylus profilometer and WLI. They indicate that roughness parameters measured by both instruments are in good agreement, with differences not bigger than 0.7, 0.7, and 1.6 μm, for R_a, R_q, and R_z, respectively. All roughness parameters depend on the direction of the analysis. Roughness parameters of hard components have higher values when sample surface is tested transversely (90°) to direction of the filling.

The slight deviations between the obtained results may be explained by the used measurement technology and surface properties of plastics. Figure 3 illustrates typical examples of the sample surfaces and explains the phenomenon of their anisotropy.

The determined square parameters sR_a and sR_q for all samples were in the range from 0.14 to 0.70 μm, while the values for sR_z were measured in the range from 1.52 to 18.55 μm (Table IV).

These results suggest that surfaces of all samples are relatively smooth, which enables the conduction of measurements for determination of the SFE.

Determination of the SFE, Parameter ΔD_{short} and Peel Force of Polymer Combinations

The SFE, its polar and dispersive component, calculated using eq. (1) and parameter D_{short}, calculated using eq. (3) are shown in Table V.

The mechanical properties as peel force for used combinations complies Table VI.

All samples have shown a completely adhesive failure (AF) according to DIN EN ISO 10365 on the entire test length. At first, the possible correlations between the SFE and the mechanical properties were investigated. Polymer TPE-E from soft components and polymer PLA Basis from hard components have the highest value of the disperse part of 36.90 and 34.28 mN/m, respectively (Table V) from which would be expected that this pair forms the strongest bonds. However, peel force for this combination is only 5.4 N. The highest adhesion is observed for the polymer TPE-E in combination with the polymer PLA where peel force is 32.3 N. The value of peel force for this combination was much lower than the peel force obtained for all combinations with polymer TPE-U as soft component, 297.8, 134.2, and 236.2 N for PLA, PLA basis, and PLA/PBS as hard components, respectively (Table VI). These results reveal that higher SFEs of the components do not lead to their enhanced

Table II. Linear Roughness Parameters for Hard Components Obtained by Profilometer and WLI

		Stylus profilometer			WLI		
Sample	Position (°)	R_a (μm)	R_q (μm)	R_z (μm)	R_a (μm)	R_q (μm)	R_z (μm)
PLA	0	0.12 ± 0.09	0.15 ± 0.01	0.87 ± 0.14	0.11 ± 0.01	0.13 ± 0.00	0.38 ± 0.10
PLA	90	0.38 ± 0.07	0.49 ± 0.06	2.48 ± 0.41	0.42 ± 0.00	0.52 ± 0.00	2.40 ± 0.21
PLA Basis	0	0.17 ± 0.00	0.23 ± 0.02	1.61 ± 0.13	0.28 ± 0.02	0.36 ± 0.00	2.31 ± 0.10
PLA Basis	90	0.40 ± 0.10	0.51 ± 0.10	2.82 ± 0.21	0.49 ± 0.02	0.61 ± 0.01	3.28 ± 0.31
PLA/PBS	0	0.21 ± 0.01	0.27 ± 0.00	1.72 ± 0.02	0.26 ± 0.00	0.33 ± 0.00	1.88 ± 0.08
PLA/PBS	90	0.35 ± 0.03	0.46 ± 0.04	2.22 ± 0.10	0.43 ± 0.03	0.54 ± 0.04	2.75 ± 0.14

Table III. Linear Roughness Parameters for Soft Components Obtained by Profilometer and WLI

		Stylus profilometer			WLI		
Sample	Position (°)	R_a (μm)	R_q (μm)	R_z (μm)	R_a (μm)	R_q (μm)	R_z (μm)
TPE-E	0	0.30 ± 0.01	0.43 ± 0.02	2.72 ± 0.13	0.13 ± 0.04	0.42 ± 0.02	3.62 ± 0.12
TPE-E	90	0.90 ± 0.30	1.28 ± 0.30	6.51 ± 0.01	0.75 ± 0.50	0.57 ± 0.02	7.30 ± 0.21
TPE-S01	0	0.63 ± 0.02	0.76 ± 0.21	4.90 ± 0.12	0.32 ± 0.07	0.40 ± 0.00	3.36 ± 0.20
TPE-S01	90	0.51 ± 0.11	0.66 ± 0.11	3.44 ± 0.30	0.28 ± 0.04	0.35 ± 0.02	2.10 ± 0.11
TPE-S02	0	0.44 ± 0.01	0.65 ± 0.07	5.65 ± 0.27	0.45 ± 0.02	0.62 ± 0.03	4.68 ± 0.13
TPE-S02	90	0.73 ± 0.01	0.95 ± 0.03	5.63 ± 0.08	0.75 ± 0.01	0.97 ± 0.01	5.58 ± 0.33
TPE-U	0	0.15 ± 0.02	0.89 ± 0.01	1.04 ± 0.01	0.15 ± 0.01	0.19 ± 0.00	0.87 ± 0.01
TPE-U	90	0.13 ± 0.03	0.17 ± 0.01	0.83 ± 0.12	0.10 ± 0.02	0.13 ± 0.00	0.62 ± 0.09

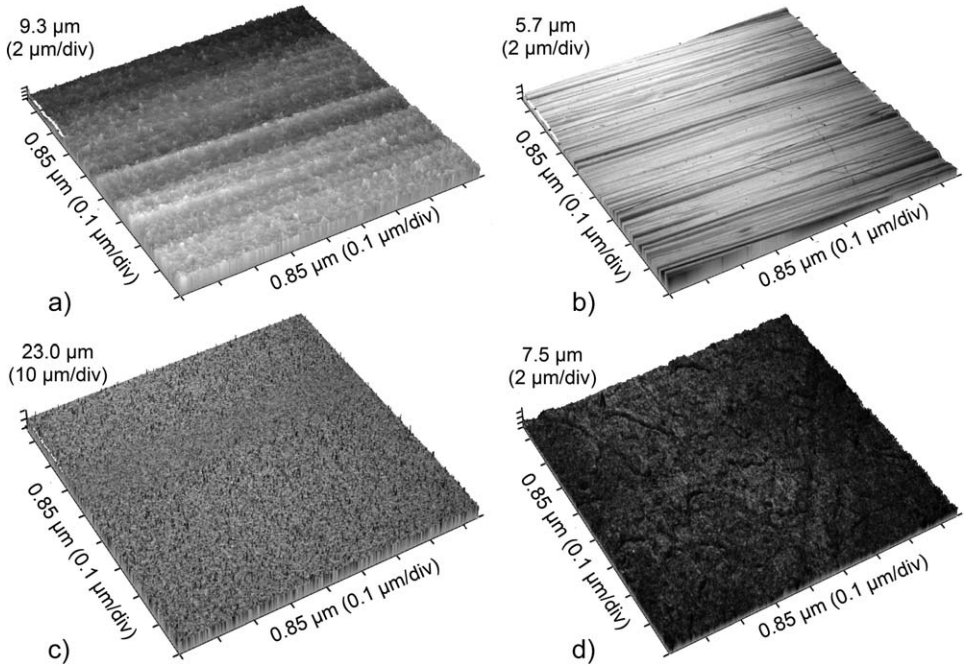

Figure 3. Topography maps of four typical surfaces obtained by WLI: (a) PLA basis, (b) PLA, (c) TPE-E, and (d) TPE-S01.

interfacial adhesion. Furthermore, from analysis of γ_S^D and γ_S^P values no correlation with the peel force can be found.

Correlation between polar ratio and peel force is also not observed, as illustrated in Figure 4. According to some papers, stronger joints are expected when polar ratio is near 1,[17,18] which is observed only for the samples where PLA Basis is the hard component. For other samples, the strongest joints are

Table IV. Surface Roughness Parameters Obtained by WLI

Sample	sR_a (μm)	sR_q (μm)	sR_z (μm)
TPE-E	0.14 ± 0.02	0.57 ± 0.04	18.55 ± 0.12
TPE-S01	0.31 ± 0.02	0.40 ± 0.04	4.38 ± 0.31
TPE-S02	0.52 ± 0.03	0.70 ± 0.02	16.85 ± 0.12
TPE-U	0.14 ± 0.02	0.18 ± 0.11	1.52 ± 0.07
PLA	0.32 ± 0.06	0.41 ± 0.22	1.58 ± 0.26
PLA Basis	0.40 ± 0.07	0.51 ± 0.09	4.98 ± 0.10
PLA/PBS	0.37 ± 0.14	0.46 ± 0.05	4.02 ± 0.27

Table V. SFE (γ_S), Disperse (γ_S^D), and polar part (γ_S^P) of the SFE and D_{short} of Polymers

Sample	γ_S (mN/m)	γ_S^D (mN/m)	γ_S^P (mN/m)	D_{short}
TPE-E	45.99 ± 0.48	36.90 ± 0.30	9.09 ± 0.19	0.07
TPE-S01	33.68 ± 0.59	33.20 ± 0.54	0.49 ± 0.05	0.23
TPE-S02	31.94 ± 0.47	29.18 ± 0.34	2.76 ± 0.13	0.38
TPE-U	37.39 ± 0.60	31.20 ± 0.40	6.19 ± 0.20	4.13
PLA	40.58 ± 0.30	31.95 ± 0.16	8.63 ± 0.14	0.77
PLA Basis	40.21 ± 0.18	34.28 ± 0.12	5.93 ± 0.06	0.84
PLA/PBS	41.09 ± 0.17	33.44 ± 0.11	7.65 ± 0.06	1.01

Table VI. Average Peel Force (N) of Hard–Soft Combinations

Soft comp. / Hard comp.	TPE-E	TPE-S01	TPE-S02	TPE-U
PLA	32.3 ± 13.1	5.7 ± 12.4	13.8 ± 2.4	297.8 ± 9.3
PLA Basis	5.4 ± 1.5	5.1 ± 1.1	6.9 ± 2.3	134.2 ± 12.0
PLA/PBS	15.0 ± 4.2	7.2 ± 2.1	11.1 ± 5.5	236.2 ± 20.1

achieved when polar ratio is 0.71 and 0.81, for combination with PLA and PLA/PBS as hard components, respectively.

Acid–base properties of the samples were determined by parameter D_{short}. All samples have D_{short} value close to 0, which is recognized as the amphoteric character of the surfaces. Only samples TPE-U and PLA/PBS have high D_{short} value of 4.16 and 1.01, respectively (Table V), which indicate pronounced acidity of the surfaces.

Parameter ΔD_{short} is further calculated using eq. (4) from D_{short} to determine the absolute difference in acidity and basicity of polymers, which is presented in Table VII.

In comparison to introduced results, relatively significant correlation between ΔD_{short} and peel force in hard–soft combination is observed, as depicted in Figure 5. Higher ΔD_{short} values indicate that differences in acid–base properties of the combined polymers are increased, which is followed by the stronger interphase interactions.

The joints between the hard and soft component are the strongest in all pairs containing the TPE-U as soft components. In these combinations ΔD_{short} has the maximum value. The highest correlation (0.996) is observed in all combinations where the PLA Basis is used as the hard component while the smallest but still good correlation (0.983) exists in combinations with the PLA as the hard component. It is also noticed that all ΔD_{short} values higher than 3 belong to combinations where peel force is higher than 150 N. However, when ΔD_{short} has value less than 3, it does not provide any information about peel force and the value of the peel force is not considered practically significant (peel force < 35 N).

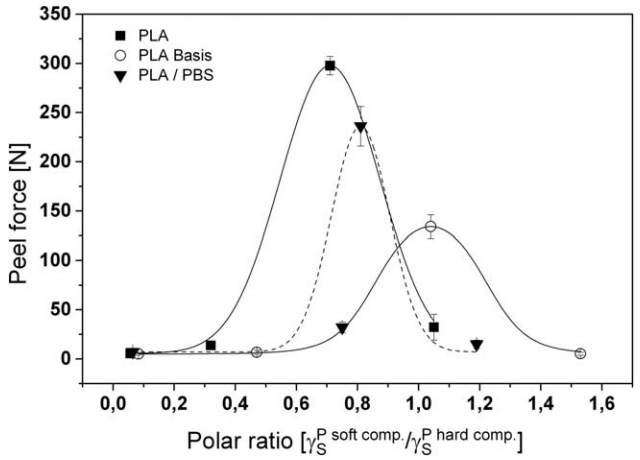

Figure 4. Correlation between the peel force and polar ratio of hard–soft combinations.

Table VII. ΔD_{short} of Hard–Soft Combinations

Soft comp. / Hard comp.		TPE-E	TPE-S01	TPE-S02	TPE-U
PLA	ΔD_{short} [(mN/m)$^{0.5}$]	0.42	0.58	1.56	4.48
PLA Basis	ΔD_{short} [(mN/m)$^{0.5}$]	0.43	0.61	0.46	3.29
PLA/PBS	ΔD_{short} [(mN/m)$^{0.5}$]	1.45	1.61	2.59	5.51

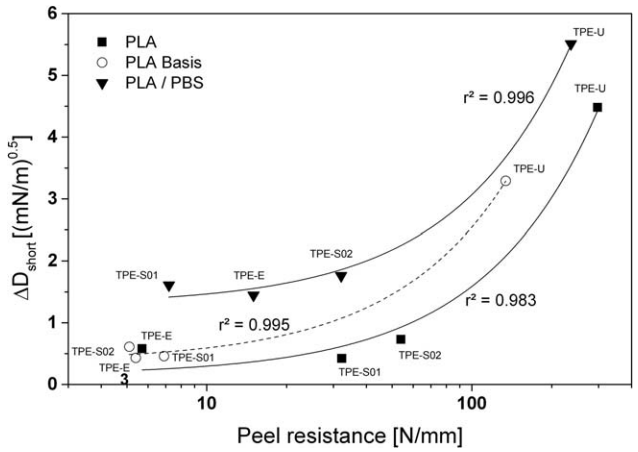

Figure 5. Linear correlation between the peel force and ΔD_{short} of hard–soft combinations presented in semi log axis (graph appear curved).

CONCLUSIONS

In this work, we address on the use of shortened version of Bergeŕs method to determine the acid–base properties of biopolymers. In the context of investigations no or very low correlation factors between the SFE (or polar parts) could be found. The difference in acidity and basicity of polymers (ΔD_{short}) is taken as the reference for the strength of the joints. Results suggest a possibility to predict the polymer interactions on this basis, since high correlation between the peel force and ΔD_{short} is observed.

Parameter ΔD_{short} reflect the chemical nature of the surface and provides useful information, e.g., for the design of the diverse adhesive systems with the desired properties.

ACKNOWLEDGMENTS

The study is supported by the Federal Ministry of Food, Agriculture and Consumer Protection, Germany (BMELV) within the framework of the Project No. 22017911 "Processing of the bio-based plastics and building the network of competence inside the FNR biopolymer network" (Verarbeitung von biobasierten Kunststoffen und Errichtung eines Kompetenznetzwerkes im Rahmen des Biopolymernetzwerkes der FNR).

REFERENCES

1. Osswald, T. A.; Menges, G. Materials Science of Polymers for Engineers, 3rd ed.; Hanser: Munich, **2012**, p 216.
2. Goodship, V. Practical Guide to Injection Moulding; Arburg: Shropshire, **2004**, p 213.
3. Goodship, G.; Love, J. C. Multi-Material Injection Moulding; Rapra Review Reports: Oxford, **2002**.
4. Bullinger, H. J. Technology Guide, Principles Applications Trends; Springer: Berlin, **2009**, p 18.
5. Yasile, C.; Zaikov, G. E. Environmentally Degradable Materials Based on Multicomponent Polymeric Systems; Koninklijke Brill NV: Leiden, **2009**, p 513.
6. Dammer, L.; Carus, M.; Raschka, A.; Scholz, L. European Bioplastics, Market Developments of and Opportunities for Biobased Products and Chemicals; Study of Nova-Institute, **2014**.
7. Fowler, G. T. Cost and Performance Evaluation Models for Comparing Multi-shot and Traditional Injection Moulding, MSc Thesis; University of Maryland, **2004**.
8. John, A.; Nagel, J.; Heinrich, G. *Open Macromol. J.* **2012**, *6*, 1.
9. Islam, A. Two Component Micro Injection Moulding for Moulded Interconnect Devices, PhD Thesis; Technical University of Denmark, Lyngby, **2008**, p 69.
10. Brecher, C. Integrative Production Technology for High-Wage Countries; Springer: Berlin, **2012**, p 500.
11. Kinloch, A. Adhesion and Adhesives, Science and Technology; Springer: University of London, **1987**.
12. Etzler, F. M.; Simmons, J.; Ladyzhynsky, N.; Thomas, V.; Maru, S. Assessment of Acid-Base Character of Polymer Surfaces from Contact Angle and Other Surface Chemical Data; In Acid-Base Interactions: Relevance to Adhesion Science and Technology, 2nd ed.; Edited by K. L. Mittal, VSP BV: Utrecht, **2000**, p 385.
13. Starostina, I. A.; Nguyen, D. A.; Burdova, E. V.; Stoyanov, O. V. *Polym. Sci. Ser. D: Glues Seal. Mater.* **2013**, *6*, 1.
14. Lobato, E. M. Determination of Surface Free Energies and Aspect Ratio of Talc, PhD Thesis. Virginia Polytechnic Institute and State University: USA, **2004**.
15. Pocius, A. V. Adhesion and Adhesives Technology, 3rd ed.; Hanser: Munich, **2012**, p 27.
16. Good, R. J.; Girifalco, L. A. *J. Phys. Chem. US.* **1960**, *64*, 561.
17. London, F. H. *Farad. Soc.* **1937**, *33*, 8b.
18. Drago, R. S.; Vogel, C. G.; Needham, T. E. *J. Am. Chem. Soc.* **1971**, *93*, 6014.
19. Gutmann, V. The Donor–Acceptor Approach to Molecular Interactions; Plenum Press: New York, **1978**, p 134.
20. Starostina, I. A.; Makhrova, N. V.; Stoyanov, O. V.; Aristov, I. V. *J. Adhes.* **2012**, *88*, 751.
21. Owens, D. K.; Wendt, R. C. *J. Appl. Polym. Sci.* **1969**, *13*, 1741.
22. Rasche, M. *Handbuch Klebtechnik.* Hanser: Munich, **2012**, p 104.
23. Lake, M. Oberflächentechnik in der Kunststoffverarbeitung: Vorbehandeln, Beschichten, Funktionalisieren und Kennzeichnen von Kunststoffoberflächen; Hanser: Munich, **2009**; Chapter 2, p 4.
24. Wojuzkij, S. S. *Colloid Polym. Sci.* **1966**, *214*, 97.
25. Berger, E. J. *J. Adhes. Sci. Technol.* **1990**, *4*, 373.
26. Kraus, E.; Baudrit, B.; Heidemeyer, P.; Bastian, M.; Stoyanov, O. V.; Starostina, I. A. *Her. Kazan Tech. Univ.* **2015**, *18*, 71.
27. Starostina, I. A.; Stoyanov, O. V.; Makhrova, N. V.; Nguyen, D. A.; Perova, M. S.; Galimzyanova, R. Y.; Burdova, E. V.; Khakimullin, Y. N. *Polym. Sci. Ser. D. Glues Seal. Mater.* **2012**, *5*, 89.
28. Kustovskii, V. Y.; Starostina, I. A.; Stoyanov, O. V. *Corros. Protect. Met.* **2006**, *79*, 930.
29. Starostina, I. A.; Stoyanov, O. V.; Bogdanova, S. A.; Deberdeev, R. J.; Kurnosov, V. V.; Zaikov, G. E. *J. Appl. Polym. Sci.* **2001**, *49*, 388.